Assessing comprehensive performance of biofilm formation and water quality in drinking water distribution systems

Li Liu, Yanyan Liu, Qingqing Lu, Guowei Chen and Gang Wang

ABSTRACT

Environmental fluctuations shape biofilm formation in drinking water distribution systems (DWDSs) and therefore distributed water quality. Yet the comprehensive performance in response to complex environmental conditions remains unclear. We investigated biofilm formation and distributed water quality under various nutrients, including chlorine concentrations and hydrodynamic conditions. Results showed that environmental fluctuations collectively induced changes in microbial propagation, which were mostly associated with turbidity variations, concentrations of total organic carbon, NH_4^+-N and soluble phosphorus compared to the other parameters. Fuzzy pattern recognition analysis integrating multiple water quality indicators revealed that low nutrient availability and addition of mild chlorine at 0.50 mg/L at 0.50 m/s flow velocity were the most favorable conditions screened for optimized comprehensive performance, while nutrient supplements yielded significant performance deterioration. These quantitative estimations offer new insights into advanced understanding of the system performance responding to often complex environmental fluctuations, essential for optimized design and practical functioning of DWDSs.

Key words | biofilm formation, drinking water distribution system (DWDS), environmental fluctuation, fuzzy pattern recognition, water quality

Li Liu
Yanyan Liu
Qingqing Lu
Guowei Chen
School of Civil Engineering,
Hefei University of Technology,
Hefei 230009,
China

Gang Wang (corresponding author)
Department of Water and Soil Sciences,
China Agricultural University,
Beijing 100193,
China
E-mail: *gangwang@cau.edu.cn*

INTRODUCTION

Quality control of the distributed water in drinking water distribution systems (DWDSs) is of great importance, as it serves as the final step for delivering potable water to consumers (Kokare *et al.* 2009; Liu *et al.* 2013). The DWDS is usually maintained at oligotrophic conditions with specific residual chlorine to minimize biofilm accumulation and therefore optimized water quality (Simões & Simões 2013). In practice, the distributed water often suffers deterioration due to violent environmental fluctuations evoking numerous interactions between microbes and their micro-habitats (Liu *et al.* 2013). Successful performance assessment and a mechanistic understanding of the underlying processes are crucial for optimized design and practical functioning of the DWDS, yet this remains elusive (Berry *et al.* 2006; Gomes *et al.* 2014).

The presence of suspended (in bulk water) and biofilm-embedded (on inner pipe surfaces) microbes in a DWDS has been recognized for several decades to degrade the quality of distributed water (Szewzyk *et al.* 2000). Facilitated by large pipeline surface area and self-produced extracellular polymeric substances, biofilm-embedded microbes often account for over 95% of the total biomass in a DWDS (Wang *et al.* 2012; Xue *et al.* 2012) Such biofilm-embedded cells take advantages, including protection against antimicrobial agents, acquisition of new genetic traits and metabolic co-operability, to survive in the often hostile

doi: 10.2166/ws.2016.134

environments of a DWDS (Kokare *et al.* 2009). Studies have revealed that undesirable microbial growth and vigorous biofilm accumulation on the water-pipe material interface could shape the micro-environments and cause severe water quality issues, such as persistence of opportunistic pathogens, acceleration of pipe corrosion, and contributions to taste, odor and color problems (Lehtola *et al.* 2006; Chowdhury 2012).

Microbial activity and the associated water quality status in a DWDS are usually governed by certain environmental factors (Lechevallier *et al.* 1990; Srinivasan *et al.* 2008). For instance, elevating flow velocity was found to promote biofilm development to some extent on the inner surface of the pipelines due to the stimulated nutrient transport and cell activity, as well as numerous interactions facilitating the uptake of microbial nutrients (Percival *et al.* 1999; Lehtola *et al.* 2006; Proulx 2010). Fluctuating flow conditions cause high level turbidity of the bulk water in a DWDS, which stimulates resuspension of the attached biomass (Lehtola *et al.* 2006). While chemical disinfectants are known to retard cell activity and propagation rates in both bulk water and biofilms of DWDSs (Simões & Simões 2013), application of high doses of disinfectants often have negative impacts on the distributed water quality due to the harmful by-products released (Wang *et al.* 2012). In addition, research has indicated that sufficient bioavailable carbon and other life-supporting substrates as well as the balance among carbon and other limiting nutrients are crucial not only to microbial growth, but also in the production of microbial extracellular polymeric substances (Chandy & Angles 2001; Sutherland 2010). This subsequently enhanced biofilm establishment, which eventually accelerated disinfectant decay and thus degraded the water quality of the DWDS. Despite these important advances, few efforts have been made to quantify the comprehensive systems performance of a DWDS (i.e., biofilm accumulation and status of the water quality yielded) in response to the often complex and variable operational conditions. These conditions are crucial for optimized design and proper functioning of a DWDS. The new aspect of this study is to provide some direct insights into how often complex and violent environmental fluctuations affect the comprehensive performance of a DWDS.

We studied the dynamics of early-stage biofilm formation in a model DWDS and the quality of the distributed water in response to variable environmental conditions, mimicking fluctuations of the hydraulic and physico-chemical conditions of a DWDS. The environmental conditions investigated included nutrient availability, chlorine disinfection and hydrodynamic conditions. In addition, a fuzzy pattern recognition technique was employed to quantify the collective effects of these environmental factors and their fluctuations on regulating the comprehensive performance of a DWDS.

MATERIALS AND METHODS

The model experimental system

The experiments were performed in a sealed model DWDS, as illustrated in Figure S1 (Supplementary information, available with the online version of this paper). The system comprises a 100.0 L plastic tank with a set of U-PVC pipes (16 mm inner diameter, ID), with removable pipe sections (16 mm ID) inserted for biofilm sampling. The water flow was driven by a centrifugal pump (PUN-200EH, Weile) and was adjusted through a flow control valve. The system was disinfected with 70% ethanol for 2 h followed by three rinses with distilled water prior to the start of the experiments (Soinia *et al.* 2002).

Feed water and solution preparation

The water used in the experiments was taken from a domestic drinking water tap in Hefei, China. To remove residual chlorine, the collected tap water was stored at room temperature ($20 \pm 2\ ^{\circ}C$) for 24 h to allow residual chlorine to decay to less than the detection limit (0.01 mg/L) (Fang *et al.* 2009) with the main characteristics listed in Table S1 (Supplementary information, available with the online version of this paper).

Chlorine stock solutions were prepared with 10.0% sodium hypochlorite (100.0 g/L, Guangfu, Shanghai) in sterile deionized water. Sodium acetate ($C_2H_3NaO_2$) was used as the carbon (C) source, and a mixture of potassium hydrogen phosphate (K_2HPO_4) and potassium dihydrogen phosphate (KH_2PO_4), at a ratio of 1:1, was added as the phosphorus (P) source (Ndiongue *et al.* 2005; Fang *et al.* 2009). The carbon and phosphorus stock solutions were prepared with

sterile deionized water, which were subsequently autoclaved at 121 °C for 15 min (Ndiongue *et al.* 2005).

Experimental setup

To quantify the effects of various environmental conditions on the comprehensive performance of DWDSs, four separate experiments (with various experimental conditions) were performed at room temperature (20 ± 2 °C) for each of the experimental scenarios, with details of the operational conditions described in the following paragraphs. The effects of flow velocity, chlorine concentration, carbon, and phosphorus sources were conducted successively as specified below.

For the flow velocity experimental scenario, pre-prepared water samples were introduced into the pipelines of the model experimental systems, with flow velocities being controlled at 0.1, 0.5, 1.0, 1.5 and 2.0 m/s. The initial chlorine concentration was identically set to 0.5 mg/L at a pH value of 7.00 (with sodium bicarbonate solution applied as a buffer medium) without any addition of carbon and phosphorus sources, mimicking the most common scenario observed in DWDSs.

Chlorine disinfection experiments were conducted at initial chlorine concentrations of 0, 0.5, 1.0, 1.5 and 2.0 mg/L with constant flow velocity set at 0.5 m/s, a pH of 7.00 and without any addition of carbon and phosphorus sources.

In the experiments for testing the effect of an exogenous carbon source, four dosages of initial sodium acetate (0, 0.25, 1.00, 2.00 and 3.00 mg C/L) were applied. Flow velocity in the pipelines was constantly maintained at 0.5 m/s with a uniform initial chlorine concentration and the pH set to 0.5 mg/L and 7.00, respectively.

For testing the effect of exogenous phosphorus, experiments were performed at initial phosphorus source dosages of 0, 10.0, 30.0, 60.0 and 100.0 μg P/L. The flow velocity inside the pipelines was constantly maintained at 0.5 m/s, with a uniform initial chlorine concentration and a pH of 0.5 mg/L and 7.00, respectively.

For all experimental scenarios, the biofilm and bulk water samples (three replications for each experiment) were collected at 24 h after incubation for estimating the densities of attached and suspended cells, the quality of the bulk water and the comprehensive performance of the DWDS.

Removal and resuspension of attached cells

The collectors of attached cells were dip-rinsed softly with sterilized distilled water to remove the loosely attached cells. A sterilized cotton wool swab was used to remove the biofilm cells on the collectors and then aseptically placed into a sterilized tube containing 10.0 mL of phosphate buffer saline. The attached cells in the tube were released into the suspension by shaking for 30 s and subsequently sonicated in a sonicator (Shumei, KQ3200E) at 40 kHz for 5 min (Gagnon & Slawson 1999).

Chemical analyses and enumeration of bacteria

Analysis of total organic carbon (TOC) was performed using a high temperature combustion method with a Shimadzu 5000 TOC analyzer (Kyoto, Japan). The turbidity was measured using a portable turbidity meter (STZ-A22C, Guangming, Wuxi). The N,N-diethyl-p-phenylenediamine method was applied to estimate chlorine concentration in the bulk water via a chlorine colorimeter (SYL-1, Xinrui, Shanghai). The total dissolved solids (TDS) was analyzed with a TDS pen (TM-03), the pH was determined with a pH meter (SG68, Mettler Toledo), and the conductivity was measured with a conductivity meter (DDSJ-308A, Leici). Nessler's reagents spectrophotometer was applied to measure the ammonia nitrogen concentration, and the dissolved phosphorus was analyzed with a Mo-Sb Anti-spectrophotometer.

The spread plate method was applied to estimate the heterotrophic plate counts (HPC) for the bulk water, inlet tap water and biofilm samples using R_2A agar medium. Prior to HPC enumeration, the plates were incubated at 22 °C for 7 days. The enumeration of the total cell counts (TCC) was performed using the acridine orange direct count according to Markku *et al.* (2004). Ten (or more) randomly selected fields (spots) were counted for each sample.

Statistical methods

Statistical differences were tested with one-way analysis of variance and the two sided t-test. Differences were considered significant when $P < 0.05$.

Fuzzy pattern recognition

The fuzzy pattern recognition analysis, an effective assessment technique, has been used for the comprehensive interpretation of water quality and other environmental data (Peng *et al.* 2010; Saadatpour *et al.* 2011). This procedure can be viewed as a two-fold task consisting of (1) learning common properties of standard sets that characterize a class and (2) deciding if a new sample belongs to the specified class by evaluating the related membership degree matrix (Ghazabfari & Rezaei 2006; Saadatpour *et al.* 2011). In this study, the fuzzy pattern technique was adopted to recognize the comprehensive performance of the DWDS as described below:

(1) Feature matrix construction. Ten characteristic indexes were selected to represent the dynamics of biofilm formation and the status of the water quality in the DWDS (i.e., turbidity, TOC, NH_4^+-N, soluble phosphorus, residual chlorine, TDS, conductivity, pH, suspended cell concentration and number of biofilm-embedded cells). Let X denote a feature matrix containing characteristic indexes of the systems performance under a set of specified experimental conditions, $X = (x_{ij})_{m\times n}$, where x_{ij} is the value of the indicator i of the sample j, with $i = 1, 2, \ldots, m$, and $j = 1, 2, \ldots, n$ (m and n are the total numbers of indicators and samples, respectively. The values of m and n were 10 and 17, respectively in this study).

(2) The classification matrix of standard values of the comprehensive performance is expressed as $Y = (y_{ih})_{m\times c}$, where y_{ih} is the standard feature value of the hth level of indicator i and can be decided by a general concept of assessment criteria, h denotes the standard level, with its value $h = 1, 2, \ldots, c$, where c is the number of standard levels (the larger the number, the higher the standard level it represents). In this study, the state of the DWDS performance was specified into five levels (i.e., $c = 5$), as seen in Table S2 (Supplementary information, available with the online version of this paper). The five levels were: good ($h = 1$), fine ($h = 2$), ordinary ($h = 3$), poor ($h = 4$) and bad ($h = 5$).

(3) Relative membership grade determination. The characteristic indexes were categorized into positive (the bigger the better) and inverse (the smaller the better) indexes. In this study, the ten selected characteristic indicators were classified as inverse indexes. The relative membership grade of the sample j (r_{ij}) as well as that of the standard feature value of the hth grade with respect to the ith index (s_{ih}) was calculated by the linear interpolation:

$$r_{ij} = \begin{cases} 0, y_{ic} \le x_{ij} \\ \dfrac{y_{ic} - x_{ij}}{y_{ic} - y_{i1}}, y_{ic} < x_{ij} < y_{i1} \\ 1, x_{ij} \le y_{i1} \end{cases}, \quad (1)$$

and

$$s_{ih} = \begin{cases} 0, y_{ih} = y_{ic} \\ \dfrac{y_{ic} - y_{ih}}{y_{ic} - y_{i1}}, y_{ic} < y_{ih} < y_{i1} \\ 1, y_{i1} = y_{ih} \end{cases}, \quad (2)$$

where y_{i1}, y_{ih} and y_{ic} represent the standard feature value of the first, hth and cth grade, respectively. Therefore, the relative membership grade matrix of the sample set, $R = (r_{ij})_{m\times n}$ as well as that of the standard set $S = (s_{ih})_{m\times c}$ can be achieved.

(4) Relative membership degree determination. The indicators of the systems' performance play different roles, which can be specifically emphasized by varying the weighing coefficients. As a consequence, the weighted generalized distance (d_{hj}) between indexes of the sample j and the corresponding standard of level h can be calculated as

$$d_{hj} = \left\{ \sum_{i=1}^{m} \left[w_i (r_{ij} - s_{ih}) \right]^p \right\}^{1/p}, \quad (3)$$

where w_i is the weighing coefficient of the ith index (with $\sum_{i=1}^{m} w_i = 1$), and p is a distance parameter (Euclidean distance is adopted, $p = 2$).

The relative membership degree of sample j at the standard level h can be determined by solving the following minimization problem (Ghazabfari & Rezaei 2006; Saadatpour *et al.* 2011):

$$Min\left\{ F(u_{hj}) = \sum_{h=a_j}^{b_j} u_{hj}^2 \cdot d_{hj}^a = \sum_{h=a_j}^{b_j} u_{hj}^2 \left\{ \sum_{i=1}^{m} \left[w_i (r_{ij} - s_{ij}) \right]^p \right\}^{2/p} \right\},$$
$$\left(\sum_{h=1}^{c} u_{hj} = 1, \text{and} 0 \le u_{hj} \le 1 \right) \quad (4)$$

where a_j and b_j are the minimum and maximum grade levels of sample j, which are acquired by comparing the relative membership grades of sample j with each row vector of matrix S. Therefore, one gets to u_{hj} $(0 \le u_{hj} \le 1)$ as

$$u_{hj} = \begin{cases} 0, & h < a_j, \text{ or } h > b_j \\ \dfrac{1}{\sum_{k=a_j}^{b_j} \left\{ \dfrac{\sum_{i=1}^{m} \left[w_i \left(r_{ij} - s_{ih} \right) \right]^p}{\sum_{i=1}^{m} \left[w_i \left(r_{ij} - s_{ik} \right) \right]^p} \right\}^{\frac{2}{p}}}, & a_j \le h \le b_j, d_{hj} \neq 0 \\ 1, & d_{hj} = 0 \end{cases} \quad (5)$$

(5) Calculation of the level feature value. The level feature value provides the basis of the comprehensive assessment with the feature vector of grade level (H) defined according to Ghazabfari & Rezaei (2006) as

$$H_j = \sum_{h=1}^{c} u_{hj} \cdot h, \quad (6)$$

where H_j is the level feature value of sample j.

RESULTS

Effects of various environmental conditions on suspended microbial growth and biofilm formation

The HPC and TCC of biofilm on inner pipe surfaces and in bulk water at 24 h after cultivation were analyzed and the results are shown in Figure 1. Specifically, a biofilm HPC number of $2.0 \times 10^3 \pm 6.7 \times 10^2$ CFU/cm^2 was estimated at a flow velocity of 0.1 m/s (Figure 1(a)). A gradually increased biofilm HPC number was observed with increasing flow velocity, which peaked to $4.0 \times 10^3 \pm 3.5 \times 10^2$ CFU/cm^2 at a flow velocity of 1.5 m/s. A further increase in flow velocity to 2.0 m/s resulted in a reduced biofilm HPC value of $1.2 \times 10^3 \pm 3.0 \times 10^2$ CFU/cm^2 (Figure 1(a)). Our results of enhanced biofilm formation by increasing flow velocity from 0.1 to 1.5 m/s are likely attributed to the facilitated mass transport and excited microbial activity (Percival *et al.* 1999; Lehtola *et al.* 2006). While at higher flow velocity of 2.0 m/s, it is deemed possible that considerably increased shear forces stimulated the detachment of biofilm cells, which contributed to the increased suspended cell density and thus reduced biofilm formation (Soinia *et al.* 2002). In contrast, flow velocity had a negative effect on suspended cell populations as shown in Figure 1(b), with the HPC value gradually decreasing from $2.9 \times 10^3 \pm 3.2 \times 10^2$ to $8.6 \pm 2.1 \times 10^2$ CFU/mL, when flow velocity was increased from 0.1 to 1.5 m/s. The suspended cell population was found to jump from $8.6 \pm 2.1 \times 10^2$ to $2.2 \times 10^3 \pm 2.0 \times 10^2$ CFU/mL when flow velocity was further increased from 1.5 to 2.0 m/s. Similar trends in the TCC values of both biofilm-embedded and suspended cells in response to the variable flow velocity value were found (Figure 1(a) and 1(b)).

The HPC and TCC profiles of biofilm and suspended cells under various chlorine concentrations are depicted in Figure 1(c) and 1(d). In the absence of chlorine, the biofilm HPC and TCC were estimated at low values of $2.0 \times 10^3 \pm 4.3 \times 10^2$ CFU/cm^2 and $1.2 \times 10^5 \pm 3.8 \times 10^3$ cells/cm^2, respectively. Both values rose considerably with increasing chlorine dosages, which peaked at values of $2.7 \times 10^3 \pm 7.2 \times 10^2$ CFU/cm^2 and $1.9 \times 10^5 \pm 3.8 \times 10^3$ cells/cm^2, respectively at a chlorine concentration of 1.0 mg/L. Further increase in chlorine dosage resulted in a continuous decrease in both biofilm HPC and TCC values reducing to $3.0 \times 10^2 \pm 5.0 \times 10^1$ CFU/cm^2 and $4.1 \times 10^4 \pm 1.9 \times 10^3$ cells/cm^2, respectively at chlorine concentration of 2.0 mg/L (Figure 1(c)). The promoted microbial surface accumulation observed under the moderate level of chlorination stress is likely attributed to microbial stress response for survival or adaptation (to biofilm-embedded life forms) encountering unfavorable conditions (Srinivasan *et al.* 2008; Simões & Simões 2013; Liu *et al.* 2015). However, higher chlorination strength certainly caused inactivation of a large amount of cells, which is responsible for the considerably reduced surface aggregation. As expected, both HPC and TCC values of suspended cells dropped from $4.0 \times 10^3 \pm 4.3 \times 10^2$ CFU/mL (HPC) and $3.9 \times 10^4 \pm 7.6 \times 10^2$ cells/mL (TCC) to $3.1 \times 10^2 \pm 9.2 \times 10^1$ CFU/mL and $4.9 \times 10^3 \pm 5.7 \times 10^2$ cells/mL, respectively, when the chlorine concentration was increased from 0 to 2.0 mg/L (Figure 1(d)). The negatively associated

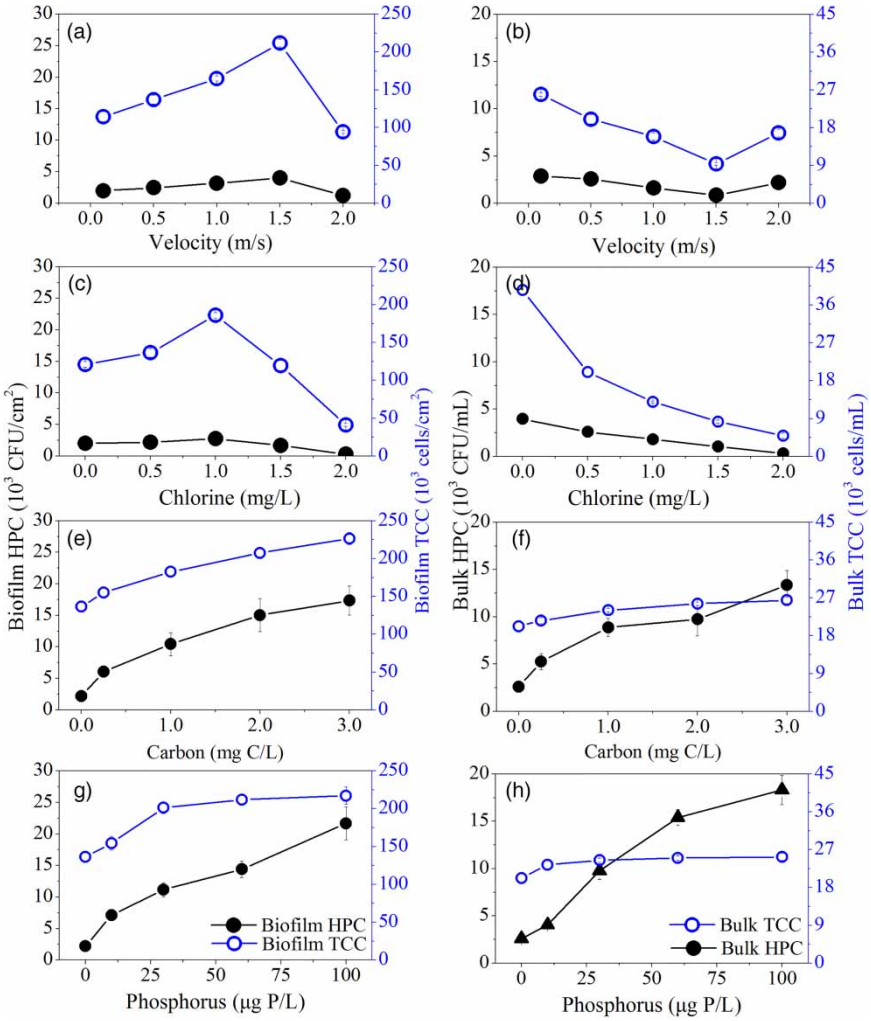

Figure 1 | The estimated HPC and TCC values (mean ± s.d., $n = 3$) of the biofilm on pipe surfaces and of the bulk water at 24 h after cultivation for (a) and (b) flow velocity variation; (c) and (d) chlorine variation; (e) and (f) carbon addition; and (g) and (h) phosphorus addition experiments.

suspended cell population with chlorine concentration provides direct evidence for dose-dependent disinfectant-induced microbial growth limitation (Wang *et al.* 2012).

Carbon addition clearly stimulated both biofilm-embedded and suspended cell propagations, as shown in Figure 1(e) and 1(f). Specifically, the estimated biofilm HPC value increased by nearly 8-fold from $2.2 \times 10^3 \pm 5.8 \times 10^2$ to $1.7 \times 10^4 \pm 2.3 \times 10^3$ CFU/cm^2 under increasing carbon addition from 0 to 3.00 mg C/L. The value for suspended HPC roughly increased 5-fold from $2.6 \times 10^3 \pm 3.0 \times 10^2$ to $1.3 \times 10^4 \pm 1.5 \times 10^3$ CFU/mL (Figure 1(e) and 1(f)). When addition of carbon was increased from 0 to 3.00 mg C/L, the TCC values for both biofilm-embedded and suspended cells continuously increased from $1.4 \times 10^5 \pm 5.6 \times 10^3$ to $2.3 \times 10^5 \pm 8.3 \times 10^3$ cells/cm^2 and from $2.0 \times 10^4 \pm 3.0 \times 10^3$ to $2.6 \times 10^4 \pm 7.8 \times 10^2$ cells/mL, respectively (Figure 1(e) and 1(f)). Similar impacts of phosphorus addition (with a range of 0 to 100.0 μg P/L) on both biofilm-embedded and suspended HPC and TCC values were found, except that the influence of phosphorus addition on the TCC value of suspended cells was less significant as shown in Figure 1(g) and 1(h). Our results show that addition of carbon and phosphorus nutrients significantly increased both biofilm-embedded and suspended cell densities in the bulk water phase, especially for HPC, which mimic the reminiscence of the above biological principles.

Effects of various environmental conditions on physical and chemical parameters of the distributed water quality

In addition to microbial indicators, physical and chemical parameters of water quality are essential to the comprehensive performance quantification of the DWDS. Table 1 lists the physical and chemical parameters of the distributed water quality under various environmental conditions. Specifically, at low flow velocity of 0.1 m/s, the turbidity level of the distributed water was estimated as 0.25 NTU, which gradually increased to 0.52 NTU as the flow velocity was elevated from 0.1 to 1.5 m/s. Further increase in flow velocity to 2.0 m/s caused only a slight reduction of the turbidity level to 0.44 NTU. The turbidity level slightly decreased from 0.37 to 0.25 NTU with the initial increase of chlorine concentration from 0 to 2.0 mg/L. In contrast, the addition of 3.00 mg C/L carbon and 100.0 μg P/L phosphorus significantly elevated the turbidity levels from 0.31 to 0.86 and 0.78 NTU ($P < 0.05$), respectively. An increase in flow velocity from 0.1 to 2.0 m/s and an increase in the initial chlorine concentration from 0 to 2.0 mg/L, gradually decreased the TOC values from 1.77 to 1.19 mg/L and from 2.04 to 1.41 mg/L, respectively. Addition of phosphorus from 0 to 100.0 μg P/L yielded a similar TOC variation from 1.73 to 1.18 mg/L when compared to the values obtained for the flow velocity scenarios. Not surprisingly, a significant increase in the TOC value from 1.73 to 3.67 mg/L was observed upon addition of carbon from 0 to 3.00 mg C/L ($P < 0.05$). The NH_4^+-N and soluble phosphorus concentrations fluctuated between 0.33 and 0.45 mg/L and between 16.4 and 32.8 μg/L, respectively when the flow velocity varied from 0.1 to 2.0 m/s. Relatively high levels of oscillations were observed for the NH_4^+-N (between 0.27 and 0.47 mg/L) and soluble phosphorus (between 16.3 and 41.2 μg/L) concentrations in response to increasing initial chlorine concentration from 0 to 2.0 mg/L. Interestingly, an increase in the addition of carbon from 0 to 3.00 mg C/L resulted in clear reductions of NH_4^+-N concentration from 0.45 to 0.26 mg/L and soluble phosphorus from 26.1 to 4.7 μg/L, respectively. An increase in the addition of phosphorus from 0 to

Table 1 | Estimated physical and chemical parameters (mean ± s.d., $n = 3$) of the bulk water at 24 h after incubation under various environmental conditions

Scenarios		Physical and chemical indexes							
Factor	Value	Turbidity (NTU)	TOC (mg/L)	NH_4^+-N (mg/L)	Soluble P (μg/L)	Residual Chlorine (mg/L)	TDS (mg/L)	Conductivity (μS/cm)	pH
Velocity (m/s)	0.1	0.25 ± 0.01	1.77 ± 0.10	0.37 ± 0.11	32.8 ± 7.2	0.00 ± 0.00	114.3 ± 0.6	214.3 ± 0.6	7.25 ± 0.02
	0.5	0.31 ± 0.03	1.73 ± 0.08	0.45 ± 0.08	26.1 ± 3.1	0.00 ± 0.00	111.3 ± 0.6	211.0 ± 0.0	7.26 ± 0.04
	1.0	0.33 ± 0.01	1.69 ± 0.08	0.43 ± 0.10	20.7 ± 2.4	0.00 ± 0.00	112.7 ± 0.6	215.0 ± 0.0	7.30 ± 0.05
	1.5	0.52 ± 0.03	1.58 ± 0.05	0.45 ± 0.12	16.4 ± 2.3	0.00 ± 0.00	113.7 ± 0.6	215.7 ± 0.6	7.70 ± 0.03
	2.0	0.44 ± 0.01	1.19 ± 0.13	0.33 ± 0.05	30.1 ± 2.2	0.00 ± 0.00	114.0 ± 1.0	216.3 ± 0.6	7.66 ± 0.05
Initial chlorine (mg/L)	0	0.37 ± 0.02	2.04 ± 0.07	0.27 ± 0.09	20.4 ± 3.1	0.00 ± 0.00	111.3 ± 0.6	207.0 ± 0.0	7.32 ± 0.03
	0.5	0.31 ± 0.03	1.73 ± 0.08	0.45 ± 0.08	26.1 ± 3.1	0.00 ± 0.00	111.3 ± 0.6	211.0 ± 0.0	7.26 ± 0.09
	1.0	0.28 ± 0.01	1.58 ± 0.14	0.47 ± 0.11	41.2 ± 4.4	0.00 ± 0.00	112.0 ± 0.6	213.7 ± 0.6	7.29 ± 0.05
	1.5	0.26 ± 0.01	1.47 ± 0.03	0.40 ± 0.03	31.6 ± 3.8	0.50 ± 0.05	113.3 ± 0.6	216.0 ± 1.0	7.50 ± 0.06
	2.0	0.25 ± 0.02	1.41 ± 0.05	0.24 ± 0.13	16.3 ± 3.6	1.00 ± 0.04	114.7 ± 0.6	219.3 ± 0.6	7.73 ± 0.03
Carbon addition (mg C/L)	0	0.31 ± 0.03	1.73 ± 0.08	0.45 ± 0.08	26.1 ± 3.1	0.00 ± 0.00	111.3 ± 0.6	211.0 ± 0.0	7.26 ± 0.03
	0.25	0.36 ± 0.01	1.80 ± 0.04	0.42 ± 0.01	14.8 ± 1.2	0.00 ± 0.00	112.0 ± 0.0	213.7 ± 0.6	7.15 ± 0.05
	1.00	0.77 ± 0.02	2.17 ± 0.09	0.36 ± 0.01	10.2 ± 6.1	0.00 ± 0.00	112.7 ± 0.6	212.7 ± 1.0	7.09 ± 0.05
	2.00	0.81 ± 0.02	2.81 ± 0.05	0.30 ± 0.01	5.8 ± 0.8	0.00 ± 0.00	114.3 ± 0.6	214.0 ± 1.5	7.13 ± 0.04
	3.00	0.86 ± 0.03	3.67 ± 0.09	0.26 ± 0.01	4.7 ± 3.1	0.00 ± 0.00	115.3 ± 0.6	215.0 ± 2.9	7.30 ± 0.06
Phosphorus addition (μg P/L)	0	0.31 ± 0.03	1.73 ± 0.08	0.45 ± 0.08	26.1 ± 3.1	0.00 ± 0.00	111.3 ± 0.6	211.0 ± 0.0	7.26 ± 0.05
	10.0	0.36 ± 0.03	1.49 ± 0.17	0.38 ± 0.02	30.3 ± 0.8	0.00 ± 0.00	112.7 ± 0.6	212.5 ± 0.6	7.36 ± 0.04
	30.0	0.68 ± 0.03	1.26 ± 0.12	0.35 ± 0.01	40.1 ± 0.6	0.00 ± 0.00	113.0 ± 0.0	213.0 ± 0.6	7.40 ± 0.09
	60.0	0.73 ± 0.01	1.22 ± 0.02	0.29 ± 0.01	67.4 ± 2.4	0.00 ± 0.00	113.3 ± 0.6	213.0 ± 0.0	7.40 ± 0.05
	100.0	0.78 ± 0.02	1.18 ± 0.05	0.23 ± 0.03	81.4 ± 0.0	0.00 ± 0.00	113.7 ± 0.6	214.3 ± 0.6	7.20 ± 0.03

100.0 μg P/L yielded a continuous increase of soluble phosphorus from 26.1 to 81.4 μg/L and a clear decrease in the estimated NH_4^+–N concentration from 0.45 to 0.23 mg/L. No detectable residual chlorine nor any minor changes in the conductivity values were found for all scenarios, except for the ones in which the initial chlorine concentrations was 1.5 and 2.0 mg/L and the residual chlorine was estimated as 0.50 and 1.00 mg/L, respectively. The environmental fluctuations had little influence on the TDS and pH, as seen with small variations in TDS value ranging from 111.3 to 115.3 mg/L and pH value ranging from 7.25 to 7.73, as observed for all scenarios.

Based on our results, nutrient availability, chlorine disinfectant and hydrodynamic fluctuations were found not only to affect microbial activity growth, but also to alter the turbidity level, TOC, NH_4^+-N and soluble phosphorus concentrations of distributed water. This in turn conspired to shape microbial propagation in both the aqueous phase and in the biofilm of the DWDS. For instance, the stimulated suspended cell growth as a result of either decreased initial chlorine concentration or increased nutrient addition was found to be associated with the elevated turbidity level, consistent with previously reported observations (Lehtola *et al.* 2006). The result has no clear correlation between the turbidity level and suspending cell density found for flow velocity variation scenarios, which is also in agreement with the findings of Lehtola *et al.* (2006). In addition, increasing flow velocity or phosphorus supplements resulted in enhanced microbial consumption of nutrients, while the application of chlorine dose yielded significant inactivation of both biofilm-embedded and suspended cells that retarded microbial propagation (Lechevallier *et al.* 1990), thereby reducing TOC values.

Comprehensive performance of biofilm formation and bulk water quality status under various experimental conditions

The experimental results presented above offer direct insights into how the environmental factors conspire to regulate early-stage biofilm formation and water quality, yet such individual parameter assessments provide limited information for understanding the comprehensive performance of the DWDS (Srinivasan *et al.* 2008). Therefore, the fuzzy pattern recognition was employed to quantify the comprehensive performance of the DWDS in response to variable experimental conditions. For convenience in calculations, the residual chlorine and pH values were converted into certain inverse indexes, expressed as the absolute difference as compared with their reference values (of residual chlorine of 0.5 mg/L and pH value of 7.00, respectively). According to the standard values listed in Table S2 (Supplementary information) and the weight vectors of 0.1, 0.1, 0.05, 0.05, 0.1, 0.1, 0.1, 0.1, 0.15, and 0.15 for turbidity, TOC, NH_4^+-N, soluble phosphorus, residual chlorine, TDS, conductivity, pH, bulk HPC and biofilm HPC, respectively, the comprehensive performance of the DWDS was specified into three levels of 'fine', 'ordinary' and 'poor' (Figure 2(a)–2(d)). For the flow velocity variation scenario, the system's performance at a flow velocity less than or equal to 1.0 m/s was specified as 'fine', with estimated performance level values ranging between 2.25 and 2.45, and an 'ordinary' performance level for a flow velocity above 1.0 m/s (Figure 2(a)). More specifically, the optimal system's performance was found to appear at a flow velocity of 0.5 m/s with an estimated level feature value of 2.25. The system's performance remained 'fine' for the entire chlorine addition scenario, except for the experimental values in the initial chlorine of 2.0 mg/L, which lowered its performance level to 'ordinary' (Figure 2(b)). In contrast, the system's performance level gradually increased from 2.25 to ~3.50 with increase in the addition of carbon and phosphorus from 0 to 3.00 mg C/L and to 100.0 μg P/L, respectively (Figure 2(c) and 2(d)). The addition of carbon or phosphorus accordingly defined the degrading performance from 'fine' (with 0 addition of carbon and phosphorus) to 'ordinary'. Of note, in adding 3.00 mg C/L, the performance level further degraded to 'poor'. These results suggested that low nutrient availability (absence of nutrient supplement) and mild chlorine addition of 0.5 mg/L at a flow velocity of 0.5 m/s were the most favorable conditions for the optimized functioning of the DWDS, while increased carbon and phosphorus addition hinder the performance of the system due to cell propagation and deterioration of the associated water quality.

To quantify the effects of the environmental conditions and their variations on the system performance of the DWDS, a relative variation estimator was initialized and

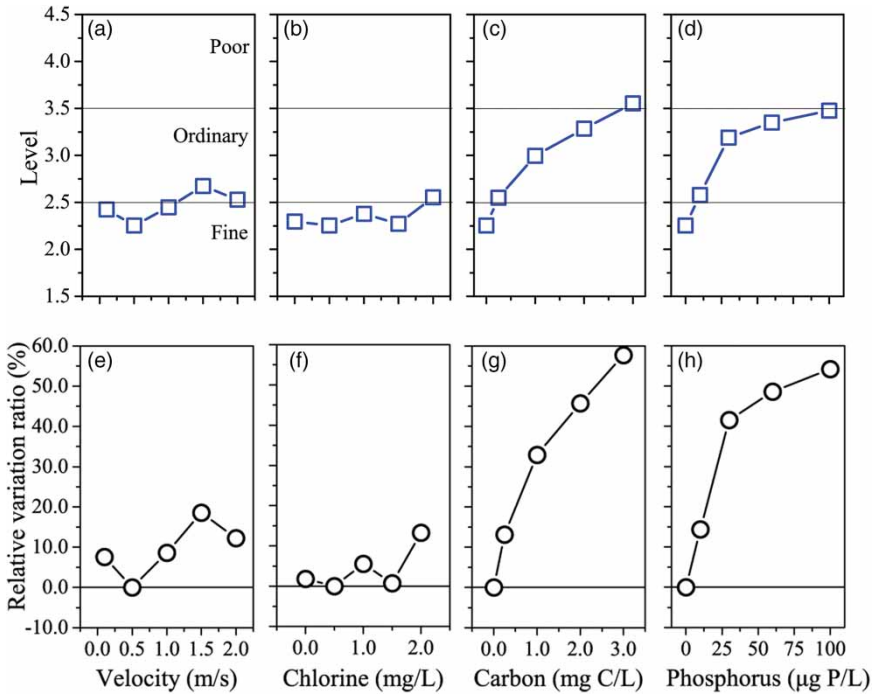

Figure 2 | The system's performance levels estimated by fuzzy pattern recognition and their relative variation ratios under various (a) and (e) flow velocities; (b) and (f) initial chlorine concentrations; (c) and (g) carbon additions; and (d) and (h) phosphorus additions.

defined as a ratio of the performance level of a testing scenario to that of the control one (of a flow velocity of 0.5 m/s, and an initial chlorine concentration of 0.5 mg/L without nutrient supplements). As shown in Figure 2(e)–2(h), relative variation ratios smaller than 18.6%, although fluctuating with increasing flow velocity and initial chlorine concentration, were found for both flow velocity and chlorine variation scenarios (Figure 2(e) and 2(f)). Rapid increase in the relative variation ratios from 0 to 57.5% and 54.2% were found when carbon and phosphorus concentrations were increased from 0 to 3.00 mg C/L and to 100.0 μg P/L, respectively. However, we also observed a relatively retarded trend for scenarios of phosphorus addition greater than 30.0 μg P/L (Figure 2(g) and 2(h)). The results indicated that addition of carbon imposed the most significant effects on the comprehensive performance of the DWDS, followed by addition of phosphorus. In contrast, flow velocity and chlorine disinfection had relatively the least influence.

System performance preferences are often required for practical operation of complex DWDSs, e.g. enhanced microbial quality for specific functions of distributed water or emphasizing of certain chemical indicators for particular industrial waters (Proulx 2010). We investigated the impact of different characteristic indexes by varying their coefficients on the assessment of system performance, as depicted (Figure 3). With equal weighing coefficients of turbidity, TOC, NH_4^+-N, soluble phosphorus, residual chlorine, TDS, conductivity, pH, bulk HPC and biofilm HPC, the system's performance level was estimated as between 1.5 and 3.5, indicating that the level of DWDS performance was either 'fine' or 'ordinary' for all scenarios (Figure 3(a)). The weighing coefficients of 0.05, 0.05, 0.05, 0.05, 0.05, 0.05, 0.05, 0.05, 0.6, and 0.0 enhanced the contribution of bulk HPC to the system's performance quantification regardless of biofilm HPC; the system's performance dropped from 'ordinary' to 'poor' for scenarios with carbon addition of 1.00–3.00 mg C/L and phosphorus addition of 25.0 and 50.0 μg P/L. For the phosphorus addition scenarios, the performance level even dropped down to 'bad' with the addition of 100.0 μg P/L. For all other scenarios, the performance was maintained at 'ordinary' level (Figure 3(b)). The weighing coefficients of 0.0, 0.0, 0.0, 0.0, 0.0, 0.0, 0.0, 0.0, 0.5, and 0.5 equally emphasized the contributions of suspended and biofilm-embedded HPC to the system's

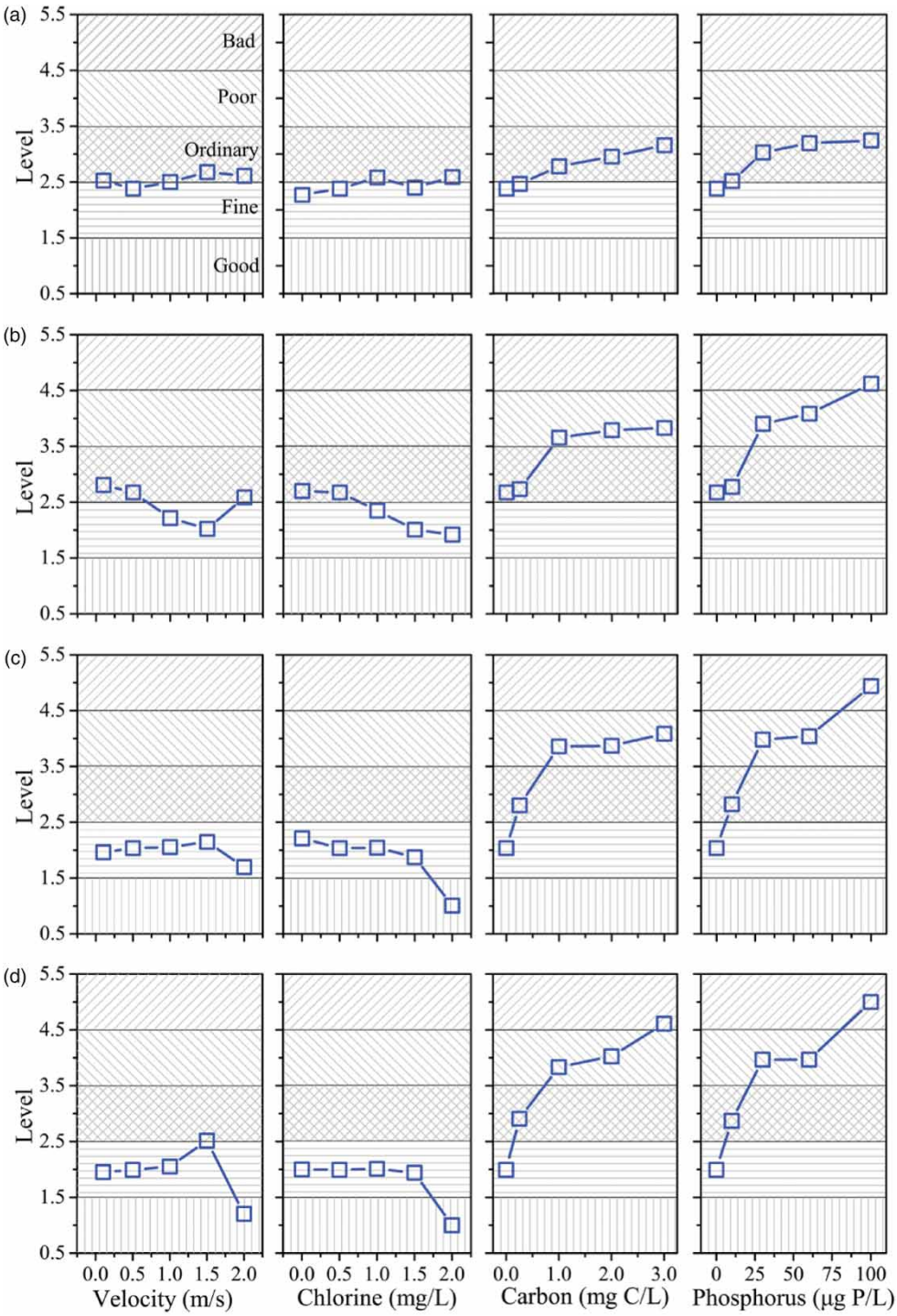

Figure 3 | The estimated performance levels under various environmental conditions with different weighing coefficients of (a) $W_1 = (0.1, 0.1, 0.1, 0.1, 0.1, 0.1, 0.1, 0.1, 0.1, 0.1)$; (b) $W_2 = (0.05, 0.05, 0.05, 0.05, 0.05, 0.05, 0.05, 0.05, 0.6, 0)$; (c) $W_3 = (0, 0, 0, 0, 0, 0, 0, 0, 0.5, 0.5)$; and (d) $W_4 = (0, 0, 0, 0, 0, 0, 0, 0, 0, 1)$.

performance while neglecting all the other parameters; the system's performance was estimated to remain at 'fine' level for all flow velocity and chlorine variation experiments, except for the scenario with initial chlorine of 2.0 mg/L, which resulted in an improved performance level from 'fine' to 'good' (Figure 3(c)). Similar trends of the system's

performance profiles were found for the carbon and phosphorus addition experiments (Figure 3(c)) compared with those shown in Figure 3(b). The contribution of only biofilm-embedded HPC to the system's performance (i.e., of weighing coefficients of 0.0, 0.0, 0.0, 0.0, 0.0, 0.0, 0.0, 0.0, 0.0, and 1.0) yielded similar estimation of performance for all scenarios as compared with those of Figure 3(c). However, a significantly improved performance level from 'fine' to 'good' was observed for the scenario of flow velocity of 2.0 m/s and a degraded performance level from 'poor' to 'bad' was seen for the experiment with carbon addition of 3.00 mg C/L (Figure 3(c) and 3(d)). Therefore, the fuzzy pattern recognition analysis suggested that the absence of nutrient addition and high chorine addition of 2.0 mg/L at flow velocity of 0.5 m/s were the optimal conditions when taking into account the weighing emphasis of performance preference for enhanced bulk HPC, biofilm HPC, or both. Meanwhile, for the equal weighing assignment, low chlorine addition of 0.5 mg/L was a potential candidate for ideal operational conditions.

CONCLUSIONS

In this study, we investigated biofilm formation and distributed water quality under various environmental conditions in a model DWDS. The results showed that flow velocity had opposing influences on the propagation of the microbial population in biofilm and bulk water, and the survival of the biofilm-embedded cells was favored over suspended counterparts at moderate velocity levels. Although the presence of chlorine suppressed the proliferation of suspended cells, moderate levels of chlorine remarkably promoted biofilm formation. Enhanced nutrient supplements favored suspended cell growth and biofilm formation. In addition, the variations in the propagation of both suspended and biofilm-embedded cells were mostly related to turbidity levels, concentrations of TOC, NH_4^+-N and soluble phosphorus compared to the other water quality parameters in response to environmental fluctuations. Comprehensive assessment revealed that oligotrophic conditions with mild chlorine of 0.50 mg/L at 0.50 m/s flow velocity were the most favorable for optimized functioning of the DWDS, while nutrient supplements resulted in significant decline of system performance.

This study provides insights for advanced understanding of the system performance in response to the complicated and variable environmental conditions of the DWDS. With the quantitative estimators, it sheds lights on the mechanistic understanding of the environmental factors and their fluctuations on shaping early-stage biofilm formation and the quality of the water yielded, which are crucial for optimized design and proper functioning of complex DWDSs (Berry *et al.* 2006).

ACKNOWLEDGEMENTS

This study was financially supported by Natural Science Foundation of China (51479046, 41401265, 51479045), the scholarship from the 'National Thousand (Young) Talents Program' from the Office of Global Experts Recruitment in China, and the Program for Changjiang Scholars and Innovative Research at the University of P. R. China (IRT0412).

REFERENCES

Berry, D., Xi, C. & Raskin, L. 2006 Microbial ecology of drinking water distribution systems. *Current Opinion in Biotechnology* **17** (3), 297–302.

Chandy, J. & Angles, M. L. 2001 Determination of nutrients limiting biofilm formation and the subsequent impact on disinfectant decay. *Water Research* **35** (11), 2677–2682.

Chowdhury, S. 2012 Heterotrophic bacteria in drinking water distribution system: a review. *Environmental Monitoring and Assessment* **184** (10), 6087–6137.

Fang, W., Hu, J. Y. & Ong, S. L. 2009 Influence of phosphorus on biofilm formation in model drinking water distribution systems. *Journal of Applied Microbiology* **106** (4), 1328–1335.

Gagnon, G. A. & Slawson, R. M. 1999 An efficient biofilm removal method for bacterial cells exposed to drinking water. *Journal of Microbiological Methods* **34** (3), 203–214.

Ghazabfari, M. & Rezaei, M. 2006 *An Introduction to Fuzzy Set Theory*. Iran University of Science and Technology Press, Tehran, Iran.

Gomes, I. B., Simões, M. & Simões, L. C. 2014 An overview on the reactors to study drinking water biofilms. *Water Research* **62**, 63–87.

Kokare, C. R., Chakraborty, S., Khopade, A. N. & Mahadik, K. R. 2009 Biofilm: importance and applications. *Indian Journal of Biotechnology* **8**, 159–168.

Lechevallier, M. W., Lowry, C. D. & Lee, R. G. 1990 Disinfecting biofilms in a model distribution system. *Journal American Water Works Association* **82** (7), 87–99.

Lehtola, M. J., Laxander, M., Miettinen, I. T., Hirvonen, A., Vartiainen, T. & Martikainen, P. J. 2006 The effects of changing water flow velocity on the formation of biofilms and water quality in pilot distribution system consisting of copper or polyethylene pipes. *Water Research* **40**, 2151–2160.

Liu, G., Verberk, J. Q. & Van Dijk, J. C. 2013 Bacteriology of drinking water distribution systems: an integral and multidimensional review. *Applied Microbiology and Biotechnology* **97** (21), 9265–9276.

Liu, L., Le, Y., Jin, J., Zhou, Y. & Chen, G. 2015 Chlorine stress mediates microbial surface attachment in drinking water system. *Applied Microbiology and Biotechnology* **99** (6), 2861–2869.

Markku, J. L., Talis, J., Ilkka, T. M., Terttu, V. & Pertti, J. M. 2004 Formation of biofilms in drinking water distribution networks, a case study in two cities in Finland and Latvia. *Journal of Industrial Microbiology & Biotechnology* **31** (11), 489–494.

Ndiongue, S., Huck, P. M. & Slawson, R. M. 2005 Effects of temperature and biodegradable organic matter on control of biofilms by free chlorine in a model drinking water distribution system. *Water Research* **39**, 953–964.

Peng, H., Zhou, H. & Li, M. 2010 Assessing water renewal of the northern coastal zone in China using a variable fuzzy pattern recognition model. *Journal of Hydroinformatics* **12** (3), 339–350.

Percival, S. L., Knapp, J. S., Wales, D. S. & Edyvean, R. G. J. 1999 The effect of turbulent flow and surface roughness on biofilm formation in drinking water. *Journal of Industrial Microbiology & Biotechnology* **22** (3), 152–159.

Proulx, F. 2010 Factors influencing public perception and use of municipal drinking water. *Water Science and Technology: Water Supply* **10** (3), 472–485.

Saadatpour, M., Afshar, A. & Afshar, M. H. 2011 Fuzzy pattern recognition method for assessing soil erosion. *Environmental Monitoring and Assessment* **180** (1), 385–397.

Simões, L. C. & Simões, M. 2013 Biofilms in drinking water: problems and solutions. *RSC Advances* **3**, 2520–2533.

Soinia, S. M., Koskinenb, K. T., Vileniusb, M. J. & Puhakka, J. A. 2002 Effects of fluid-flow velocity and water quality on planktonic and sessile microbial growth in water hydraulic system. *Water Research* **36**, 3812–3820.

Srinivasan, S., Harrington, G. W., Xagoraraki, I. & Goel, R. 2008 Factors affecting bulk to total bacteria ratio in drinking water distribution systems. *Water Research* **42**, 3393–3404.

Sutherland, I. 2010 Biofilm exopolysaccharides: a strong and sticky framework. *Microbiology* **147**, 3–9.

Szewzyk, U., Szewzyk, R., Manz, W. & Schleifer, K. H. 2000 Microbiological safety of drinking water. *Annual Review Microbiology* **54**, 81–127.

Wang, H., Masters, S., Hong, Y., Stallings, J., Falkinham, J. O. & Edwards, M. A. 2012 Effect of disinfectant, water age, and pipe material on occurrence and persistence of *Legionella, mycobacteria, Pseudomonas aeruginosa*, and two amoebas. *Environmental Science & Technology* **46** (21), 11566–11574.

Xue, Z., Sendamangalam, V. R., Gruden, C. L. & Seo, Y. 2012 Multiple roles of extracellular polymeric substances on resistance of biofilm and detached clusters. *Environmental Science & Technology* **46** (24), 13212–13219.

First received 16 May 2016; accepted in revised form 4 August 2016. Available online 12 August 2016